Phase organization of circadian oscillators in extended gate and oscillator models

Gang Zhao

Institute of Complex Bio-dynamics, Jiangxi Blue Sky University, Nanchang, Jiangxi, 330098, People's Republic of China

Abstract

The suprachiasmatic nuclei (SCN) control daily oscillations in physiology and behavior. The gate-oscillator model captures function heterogeneity in SCN and has been successful in reproducing many features of SCN. This paper investigates the mechanism of phase organization in the gate-oscillator model and finds that only stable fixed points of the phase transition function are essential to phase organization. Extending the model with a dead zone of the phase transition function and the propagation delay of the gate signal which represents the spatial structure of SCN, the author discusses how the experimentally reported phase distribution, including phase splitting of

animals in LL condition, and fixed phase difference between neurons of SCN could be understood in the framework of the gate-oscillator model. The extended model provides two mechanisms for phase splitting and gives a testable prediction that the two clusters of neurons of the phase splitting animal differ in their inherent periods.

Introduction

The mammalian circadian pacemaker is located in the suprachiasmatic nuclei (SCN) of the anterior hypothalamus [1, 2]. The molecular mechanism for sustained oscillation of clock genes and their protein products are being identified [3, 4]. It's now known that the clock genes produce ~24 hr oscillations in individual cells through interlocked transcription-translation feedback loops. However, how individual cells are organized to create a robust and adaptive rhythmic output and control behavioral and physiological rhythms are less well understood [5]. For example, there is evidence which suggests that SCN is composed of two coupled equivalent, but functionally distinct oscillators termed “morning” and “evening” oscillators, although the mechanism and location of them are controversial [6-10]. It is now well established that SCN is composed of multiple heterogeneous neuron

populations that differ in their peptidergic phenotype, responsiveness to light, pattern of gene expression, electronical activity phase and their function [11].

Classically, SCN is subdivided into a dorsalmedial shell and a ventrolateral core [12, 13]. The core of SCN comprises cells that are non-rhythmic or weakly rhythmic in relevant clock genes expression [14, 15] or their firing rate [16] but receive direct photo inputs [17]. Destruction of these cells leads to arrhythmic behavior. Moreover, the shell SCN becomes arrhythmic because of lacking synchrony [18, 19]. These findings have motivated Antle et al to propose the gate and oscillator model [20, 21], in which the gate cells (core SCN neurons) send resetting signals, which make the shell neurons' phase more compact, to the oscillator cells (shell SCN). The gate is activated if the output of oscillator cells exceeds some threshold. The gate and oscillator model differs from other mathematical models of SCN by representing the functional heterogeneity in SCN while it neither requires nor excludes global or local coupling between oscillator cells which is the subject of other models.

The gate and oscillator model has been successful in explaining not only the coupling between the rhythmic and non-rhythmic cells in SCN that is essential to the coherent circadian tissue output, but also in explaining the

light entrainment and phase-response curve [5]. It is impressive that such a simple model could account for the complex behavior of SCN in many aspects [22]. Moreover, a strong support for this model is the presence of anti-phase neurons within the shell SCN [6, 19, 23, 24], which is difficult to explain by coupling only [25]. By replacing the original linear phase resetting function with a sigmoid one, Yan et al. have modeled the anti-phase populations of neurons in the gate and oscillator model [6]. Although a mathematical model of global coupling could also bring about cells that have a phase difference of about 12 hr [26], it falls shot in that the portion of anti-phase cells are very small because only neurons that have extremely long or short period are anti-phase.

While achieving considerable success, the detailed mechanism of how the gate cells organize oscillator cells' phase and how the specific form of the phase resetting function, such as a long dead zone [22], would influence the phase distribution of oscillator cells are not clear. How oscillator cells would respond to the gate signals is not known now. But some theoretical [22] and experimental [27] results have provided indirect support for a phase resetting function either with or without dead zone. It may appear reasonable to

suspect that the response of oscillator cells to the gate signal may be plastic under different conditions.

Furthermore, a simplification of the original model is that the oscillator cells are homogeneous, in the sense of responding to the resetting signal. Some experimental results have emphasized the importance of spatial organization of the shell SCN in understanding the circadian phenomena. For example, the dorsal cells that are near to the third ventricle express vasopressin mRNA (a clock controlled gene) and Period 1 gene first, then the expression spread to the central part after 4-8 hours [19, 28]. The time window of expressing vasopressin and Per1 mRNA of those preceding cells are longer than that of the ventral cells. It is suggested that gate cells may directly contact those preceding cells. Meanwhile, the two candidate gate signal, vasoactive intestinal polypeptide (VIP) and gastrin-releasing peptide (GRP), may act in a diffusible manner, as SCN explants can initiate and maintain coherent oscillations in cultures 0.5 mm away [29]. Although the mechanism for the slow spread of gene expression in the shell SCN is now not known, it is clear that the spatial organization exists not only in the core-shell (gate-

oscillator) relationship, but also in the shell (oscillators). And it is also evident that this organization is plastic under different conditions [24, 30-32].

The author investigates in this paper the detailed mechanism of how the gate organizes the phase of oscillator cells, especially the effects of the dead zone of the single cell phase resetting function. It is found that the oscillator cells' phases are separated into two clusters, the distance between which equals approximately the dead zone of the single cell resetting function. The cluster that resets earlier consists of oscillators with relatively small period; while the other cluster is made up of oscillators with relatively long period. And, by incorporating propagation delay of the resetting signal, which represents the spatial organization in the shell SCN in an unsophisticated way, the author discusses how the gate and oscillator model could bring about phase splitting and other form of phase distribution that have been reported in relevant experiments.

The rest part of the paper is organized as follows. The next section is devoted to introducing the model and parameters. Then, simulation results are presented in the flowing section step by step. The last part is dedicated to some discussions and conclusions.

Model and method

The model consists of N=2000 oscillator cells and one gate. The gate is activated by strong enough output of the oscillators, i.e., if the overall output of oscillator cells is above a predefined threshold. The activated gate then sends resetting signals to oscillator cells. Each oscillator cell receives the signal either instantly or after a specified delay time. Once receiving the resetting signal, the oscillator cell responds to the signal by changing its phase according to the so-called phase resetting function.

Single oscillator cells

The single oscillator cell evolves according to the following equations which are the same as in [20]:

$$\frac{dr}{dt} = -\varepsilon\alpha r\cos(\theta)^2[-1+\beta r^2\cos(\theta)^2] \quad (1a)$$

$$\frac{d\theta}{dt} = \frac{\alpha}{2}[-2+2\beta\varepsilon r^2\cos(\theta)^3 r^2\sin\theta - \varepsilon\sin(2\theta)] \quad (1b)$$

where ε is the stiffness coefficient, α sets the frequency of the oscillator, β is a scaling coefficient and the polar coordinates are defined by the angle ϑ and the radius r. In all simulations, ε is set to 0.2; β is set to 1, and α is determined

by $\frac{2\pi}{T}$, where *T* is the inherent period of each oscillator. The output of a single oscillator cell *i* at time *t* is given by

$$x_i = r_i(t) * \cos\theta_i(t) \qquad (2).$$

The phase of each oscillator is considered to be its current ϑ value.

The network of oscillator cells

There are 2000 oscillator cells in the model. The period of each oscillator is picked from a normal distribution with the mean being 23.5 hr and the standard deviation being 1.28 hr. These two values are from multielectrode recordings from dispersed SCN neurons [33]. The initial phase of each oscillator is uniformly distributed between 0 and π, i.e., about 12 hr. The initial value of *r* is set to 0.75 for all the oscillator cells.

In simulations, the phase of each oscillator would change according to the so-called phase resetting function upon the arrival of the resetting signal which is sent out by the gate. The resetting signal may take a period of time, which is termed as signal delay, to reach its targets. Since there are no relevant data in the literature about the distribution form of signal delay, it is assumed to be a *uniform distribution* as a starting point. The signal delay of

each oscillator is selected from the internal [0 *delay_max*], where *delay_max* is a parameter that sets the maximum signal delay of the oscillator cells. Experimental results suggest that *delay_max* is about 8 hr [28] or 15 hr [19]. Since the simulations are integrated with a fixed time step of *dt*, the delays are constrained to be multiples of *dt*. For example, if *delay_max* is set to 2 hr and *dt*=0.5 hr, the signal delay of oscillators could only be one of following: (0, 0.5, 1, 1.5, 2).

The overall output of oscillator cells is the mean of the current output of single oscillators:

$$X(t) = \frac{1}{N}\sum_{i=1}^{N} x_i(t) \qquad (3)\,.$$

The Gate and the phase resetting function

The gate could send out the resetting signal if the overall output of the oscillator cells exceeds certain threshold and at the same time, a latent period has expired. The gate threshold is set to 0.1 all through the paper. The gate latency is 20 hr as in the original model, in other words, the gate will be silent for 20 hr after activation even if the overall output of oscillator cells exceeds the threshold.

The resetting signal, once reaching an oscillator cell, could reset its phase according to the so-called phase resetting function. In the original model, the phase resetting function is a linear function whose ability of resetting is characterized by its slope [21]. The effect of phase resetting could also be represented by the phase transition function which is adopted in this paper. The phase transition function considered in this paper is plotted in Fig. 1, which consists of four line segments. The interval from 0 to θ_0 is the so called dead zone; θ_0=0 means that the phase resetting function has no dead zone. θ_1 and θ_2 are the first and last quartiles of the interval from θ_0 to 2π, respectively. The maximal phase change is *h* that occurs at θ_1 or θ_2. The parameter *h* indicates the phase resetting capability of the phase transition function. The value of h is set to 4 hr unless specifically assigned.

If θ_0=0, i.e., there is no dead zone, the phase transition function intersects the x-axis at two points: 2π (0) and θ_u, the latter one being the midpoint of θ_1 and θ2. These two points are fixed point of the phase transition function, the former one stable and the latter unstable. If $\theta_0 \neq 0$, the fixed points of the phase transition function are infinity, among which three points

are special. One is θ_0, another is θ_u, the third one is 2π (0). Among these fixed points, the first and the last one are stable.

The simulation

The ordinary differential equations of 2000 oscillators are integrated via the Euler forward scheme with a time step of 0.5h. The phase of each oscillator just before and after resetting, overall phase distribution are analyzed in particular.

Results

The case of no dead zone

As stated previously, a phase transition function that has no dead zone gives rise to two fixed points, one is 0 (2π), the other is $\theta_u=\pi$. By a simple stability analysis, one can get the conclusion that θ_u is unstable while 0 (2π) is stable. The stability property has significant influence on the overall phase distribution.

Fig. 2 shows three examples, with the value of *h* set to 8 hr (left), 6 hr (middle) and 4 hr (right) respectively. The top row shows the overall output, the middle row shows the standard deviation of phases. It is evident, and not

surprising, that larger value of *h* leads to more coherent overall output with larger amplitude. The bottom row shows the phase-period relationship (left sub-panel) and the corresponding distribution of the phases (right sub-panel) at three time points: just before the 20^{th} reset (blue), just after the 20^{th} reset (red) and 10 hr after the 20^{th} reset (black). Three points are worth noting in regard to these phase-period relationship and the corresponding phase distributions. First, oscillators with extreme periods could not be organized by the gate. This is more evident in the case of limited resetting capability when *h*=4 hr. Second, when the gate is activated, those organized oscillators are near the stable fixed point of the phase transition function. The phase-period relationship is approximately a line. After reset, the slope of this line becomes smaller (even become negative in the case of strong resetting capability when *h*=8 hr). Then, the slope progressively becomes larger until the next time of resetting. Lastly, the phase distribution, induced by a strong resetting capability, is limited in a small range all the time. Therefore, those organized oscillators keep approximately constant phase relationships (Fig. 3 red). In the case of a weak gate, the phase distribution is much wider, but the phase difference between two randomly chosen unorganized oscillators is not limited in a small range (Fig. 3 blue). Experimental results suggest that

although the overall phase distribution is wide [19, 24], the phase difference between individual neurons is conserved [19]. Therefore, it is hard to explain those experimental results within such a simple gate-oscillator model. Moreover, the period of the overall output, which is indicated by the intersection point of the red and blue line in the phase-period plot, deviates considerably from the mean of individual oscillators.

Effects of the dead zone

If the phase transition function features a dead zone, there are three special fixed points of the phase transition function, 2π (0), θ_0 and θ_u. By a simple stability analysis, one comes to the conclusion that the first two are stable and the last one is unstable. The introduction of an extra stable fixed point changes the overall phase distribution from unimodal to bimodal form, which is exemplified in Fig. 4 with θ_0=6 hr (left) and θ_0=10 hr (right). The parameter *h* is set to its default value 4 hr in both cases in Fig. 4.

The first row of Fig. 4 plots overall output; the second row plots the corresponding standard deviation of phases. By comparing the two cases, it is obvious that the longer dead zone compromises the coherence of the overall output. However, this is not because more oscillators are unorganized. The

phase-period relationship just before (blue) and after (red) the 20th reset are presented in the third and bottom row in Fig. 4, with the corresponding phase distributions on the right sub-panel. It is found that the phase distribution splits into two clusters centered around the two stable fixed points of the phase transition function. The two clusters differ in their oscillators' period. One cluster runs faster than the overall period while the other is slower. The resetting effects for the two clusters are also different. The phases of those relatively faster oscillators are delayed by the gate while the phases of those slower oscillators are advanced by the gate. There also exist some oscillators that are not influenced by the gate because their phases are in the dead zone when the gate is active. The period of these uninfluenced oscillators coincide with the period of the overall output, which is now much closer to the mean of period of individual oscillators (compared with the case in Fig. 2). To confirm that the two clusters are separated by a distance equaling the dead zone, their relationship is shown in Fig. 5.

Another feature worth mentioning is suggested by comparing Fig. 4 with the case in Fig. 3 left column, where the parameter *h* is also 4 hr. In the left column of Fig. 3, there are about 40% oscillators that are unorganized. While

by introducing a dead zone, this portion is largely diminished. This is not so surprising if one realizes that only stable fixed points are essential to organize the oscillators' phase. By introducing a dead zone, an extra stable fixed point comes into being.

Effects of signal delay

Since the *mPer1* and *mPer2* gene expression in shell SCN follows specific spatial-temporal pattern [19, 28], and the phase reset effect induced by light is carried out by activating *mPer1* and mPer2, the author tries to model this topographical complexity of SCN by the propagation delay of the resetting signal. It is convenient to include signal delay in the gate-oscillator scheme while it is not very easy to do so in a model that relies on local or global coupling only.

Fig. 6 gives an example of phase-period relationship (left), phase distribution (middle) and phase-delay relationship (right) when signal delay is considered. The signal delay of each oscillator is picked from a uniform distribution in the internal from zero to 3 hr, i.e., *delay_max*=3. The length of the dead zone is 11 hr and other parameters are set to their default values as

stated in the model and method section. The time of this snapshot is 12 hr after the 20^{th} reset of oscillator cells whose signal delay is zero.

The overall bimodal distribution is not changed very much by signal delay, although the peaks are not as acute as in Fig. 4 where signal delay is not considered. The phase of each oscillator, at the time just before its reset, is around one of the stable fixed points of the phase transition function, the faster around 0 (2π) while the slower around θ_0. However, since oscillators are reset one group after another rather than simultaneously, the phases in each cluster are divided into groups according to their signal delay. Hence each cluster has a size of at least *delay_max*. This situation is not reflected by the overall phase distribution because of overlapping, but it is clear in the phase-period and phase-delay plot. In such a scheme, the phase of each oscillator is determined by three factors: the dead zone, its inherent period and its signal delay.

The two clusters in the overall distribution in Fig. 6 appear to having same number of oscillators and having the same structure. However, it is not the necessary result if *delay_max* is longer than the dead zone of the phase transition function. In such a case the two clusters are not well separated

because their distance is not longer than their sizes. Fig. 7 shows such a case where the dead zone is 7 hr while *delay_max* is 10 hr.

Discussion

The gate-oscillator model suggests that if a daily resetting signal is working, SCN could sustain rhythmicity in the DD condition and be entrained by LD cycle [20, 21]. A detailed investigation into the mechanism of phase organization in this paper discovers that the stable fixed points (or point) of the phase transition function are of crucial importance. Those organized cells stay around stable fix points (or point) when being reset by the gate. This finding provides the basis for understanding other complex behavior of SCN.

If incorporating a dead zone into single cell phase transition function and signal delay on the network level, the extended gate-oscillator model could account for at least two features of SCN. First, the phase of individual cells is distributed in a broad range while phase difference between specific pair of cells is confined in a limited range. This could be the result of a broadly distributed signal delay or the interplay between *delay_max* and the dead zone. Moreover, some experimentally reported phase distribution, such as Fig. 2(B) in [19], could be reproduced in the model by intricately tuning the mean

and variance of a normally distributed signal delay (data not shown). Second, the model predicts there are two ways to reproduce the phase splitting behavior of animals in LL condition. The LL condition may extend the dead zone to divide the previously unimodal distribution into bimodal or shorten the range of signal delay which otherwise would mask the bimodal distribution. A prediction with respect to phase splitting by the model is that the two clusters differ in their periods if isolated. One is shorter than the overall period and another is longer. As a consequence, the faster one is delayed and the slower one is advanced by the gate signal.

The simulations in the extended gate-oscillator models have shown that three factors are crucial to the phase organization of SCN neurons, their inherent period, their responsiveness to the resetting signal and their signal delay. These factors are assumed to be constant for individual oscillators and independent of each other in the present study. The circadian clock located in SCN may make use of their correlation and plasticity to build a more complex and adaptable time-keeping device.

Figure Legend:

Figure 1: An example of the phase transition function. The x-axis is the phase at which the reset takes place. The y-axis is the phase transition. The dead zone is between 0 and θ_0.

Figure 2: Overall output (top), standard deviation of phase (middle) and phase organization with different value of *h* plotted in different column when the dead zone is not present. Blue: just before the 20th reset; Red: just after the 20th reset; Black: 10 hr after the 20th reset.

Figure 3: The evolution of phase difference between two randomly chosen organized oscillators (Red) and unorganized oscillators (Blue) when *h*=4 hr.

Figure 4: Overall output (top), standard deviation of phase (middle) and phase organization with a dead zone of 6 hr (left) and 10 hr (right). Blue: just before the 20th reset. Red: just after the 20th reset.

Figure 5: The distance between two clusters are plotted as a function of the length of the dead zone when *h*=4. The distance is taken as the span between the peaks of each cluster when the phase-axis is divided into 24 bins.

Figure 6: The phase-period relationship (left), corresponding phase distribution (middle) and phase-delay relationship (right) after 12 hr of the

20^{th} reset. The dead zone is 11 hr and *delay_max* is 3 hr. The histogram of the phase distribution contains two clusters, each divided into 7 sloping lines in the phase-period plot.

Figure 7: Cluster overlapping due to a larger *delay_max.* The dead zone is 7 hr and *delay_max* is 10 hr.

1. Weaver, D.R. The Suprachiasmatic Nucleus: A 25-Year Retrospective. *J Biol Rhythms* **13**, 100-112 (1998).
2. Reppert, S.M. & Weaver, D.R. MOLECULAR ANALYSIS OF MAMMALIAN CIRCADIAN RHYTHMS. *Annual Review of Physiology* **63**, 647-676 (2001).
3. Hastings, M.H. & Herzog, E.D. Clock Genes, Oscillators, and Cellular Networks in the Suprachiasmatic Nuclei. *J Biol Rhythms* **19**, 400-413 (2004).
4. Okamura, H. Clock Genes in Cell Clocks: Roles, Actions, and Mysteries. *J Biol Rhythms* **19**, 388-399 (2004).
5. Indic, P., Schwartz, W.J., Herzog, E.D., Foley, N.C. & Antle, M.C. Modeling the Behavior of Coupled Cellular Circadian Oscillators in the Suprachiasmatic Nucleus. *JOURNAL OF BIOLOGICAL RHYTHMS* **22**, 211 (2007).
6. Yan, L., Foley, N., Bobula, J., Kriegsfeld, L. & Silver, R. Two antiphase oscillations occur in each suprachiasmatic nucleus of behaviorally split hamsters. *Journal of Neuroscience* **25**, 9017-9026 (2005).
7. de la, H., Meyer, J., Carpino, A. & Schwartz, W. Antiphase oscillation of the left and right suprachiasmatic nuclei. *SCIENCE* **290**, 799-801 (2000).
8. Stoleru, D., Peng, Y., Agosto, J. & Rosbash, M. Coupled oscillators control morning and evening locomotor behaviour of Drosophila. *NATURE* **431**, 862-868 (2004).
9. Jagota, A., Horacio, O. & Schwartz, W. Morning and evening circadian oscillations in the suprachiasmatic nucleus in vitro. *NATURE NEUROSCIENCE* **3**, 372-376 (2000).
10. Grima, B., Chélot, E., Xia, R. & Rouyer, F. Morning and evening peaks of activity rely on different clock neurons of the Drosophila brain. *NATURE* **431**, 869-873 (2004).

11. Antle, M. & Silver, R. Orchestrating time: arrangements of the brain circadian clock. *TRENDS in Neurosciences* **28**, 145-151 (2005).
12. Moore, R.Y. & Silver, R. Suprachiasmatic Nucleus Organization. *Chronobiology International* **15**, 475-487 (1998).
13. Moore, R., Speh, J. & Leak, R. Suprachiasmatic nucleus organization. *Cell and Tissue Research* **309**, 89-98 (2002).
14. Dardente, H., Poirel, V.-J., Klosen, P., Pévet, P. & Masson-Pévet, M. Per and neuropeptide expression in the rat suprachiasmatic nuclei: compartmentalization and differential cellular induction by light. *Brain Research* **958**, 261-271 (2002).
15. Hamada, T., LeSauter, J., Venuti, J. & Silver, R. Expression of Period Genes: Rhythmic and Nonrhythmic Compartments of the Suprachiasmatic Nucleus Pacemaker. *Journal of Neuroscience* **21**, 7742 (2001).
16. Jobst, E. & Allen, C. Calbindin neurons in the hamster suprachiasmatic nucleus do not exhibit a circadian variation in spontaneous firing rate. *European Journal of Neuroscience* **16**, 2469-2474 (2002).
17. Karatsoreos, I.N., Yan, L., LeSauter, J. & Silver, R. Phenotype Matters: Identification of Light-Responsive Cells in the Mouse Suprachiasmatic Nucleus. *J. Neurosci.* **24**, 68-75 (2004).
18. LeSauter, J. & Silver, R. Localization of a Suprachiasmatic Nucleus Subregion Regulating Locomotor Rhythmicity. *J. Neurosci.* **19**, 5574-5585 (1999).
19. Yamaguchi, S*., et al.* Synchronization of Cellular Clocks in the Suprachiasmatic Nucleus. *SCIENCE* **302**, 1408-1412 (2003).
20. Antle, M.C., Foley, N.C., Foley, D.K. & Silver, R. Gates and Oscillators II: Zeitgebers and the Network Model of the Brain Clock. *JOURNAL OF BIOLOGICAL RHYTHMS* **22**, 14-25 (2007).
21. Antle, M.C., Foley, D.K., Foley, N.C. & Silver, R. Gates and Oscillators: A Network Model of the Brain Clock. *JOURNAL OF BIOLOGICAL RHYTHMS* **18**, 339 (2003).
22. Welsh, D.K. Gate Cells See the Light. *J Biol Rhythms* **22**, 26-28 (2007).
23. Schaap, J*., et al.* Heterogeneity of rhythmic suprachiasmatic nucleus neurons: Implications for circadian waveform and photoperiodic encoding. *Proceedings of the National Academy of Sciences* **100**, 15994-15999 (2003).
24. Quintero, J., Kuhlman, S. & McMahon, D. The Biological Clock Nucleus: A Multiphasic Oscillator Network Regulated by Light. *Journal of Neuroscience* **23**, 8070-8076 (2003).
25. Indic, P., Schwartz, W.J. & Paydarfar, D. Design principles for phase-splitting behaviour of coupled cellular oscillators: clues from hamsters with 'split' circadian rhythms. *J. R. Soc. Interface* **5**, 873-883 (2008).

26. Gonze, D., Bernard, S., Waltermann, C., Kramer, A. & Herzel, H. Spontaneous Synchronization of Coupled Circadian Oscillators. *Biophysical Journal* **89**, 120-129 (2005).
27. Liu, C. & Reppert, S.M. GABA Synchronizes Clock Cells within the Suprachiasmatic Circadian Clock. *Neuron* **25**, 123-128 (2000).
28. Hamada, T., Antle, M.C. & Silver, R. Temporal and spatial expression patterns of canonical clock genes and colck-controlled genes in the suprachiasmatic nucleus. *European Journal of Neuroscience* **19**, 1741 (2004).
29. Prolo, L.M., Takahashi, J.S. & Herzog, E.D. Circadian Rhythm Generation and Entrainment in Astrocytes. *J. Neurosci.* **25**, 404-408 (2005).
30. vanderLeest, H.T., Rohling, J.H.T., Michel, S. & Meijer, J.H. Phase Shifting Capacity of the Circadian Pacemaker Determined by the SCN Neuronal Network Organization. *Plos One* **4**, e4976 (2009).
31. Inagaki, N., Honma, S., Ono, D., Tanahashi, Y. & Honma, K.-i. Separate oscillating cell groups in mouse suprachiasmatic nucleus couple photoperiodically to the onset and end of daily activity. *Proc. Natl. Acad. Sci. USA* **104**, 7664-7669 (2007).
32. Brown, T.M. & Piggins, H.D. Spatiotemporal Heterogeneity in the Electrical Activity of Suprachiasmatic Nuclei Neurons and their Response to Photoperiod. *J Biol Rhythms* **24**, 44-54 (2009).
33. Herzog, E.D., Aton, S.J., Numano, R., Sakaki, Y. & Tei, H. Temporal Precision in the Mammalian Circadian System: A Reliable Clock from Less Reliable Neurons. *J Biol Rhythms* **19**, 35-46 (2004).

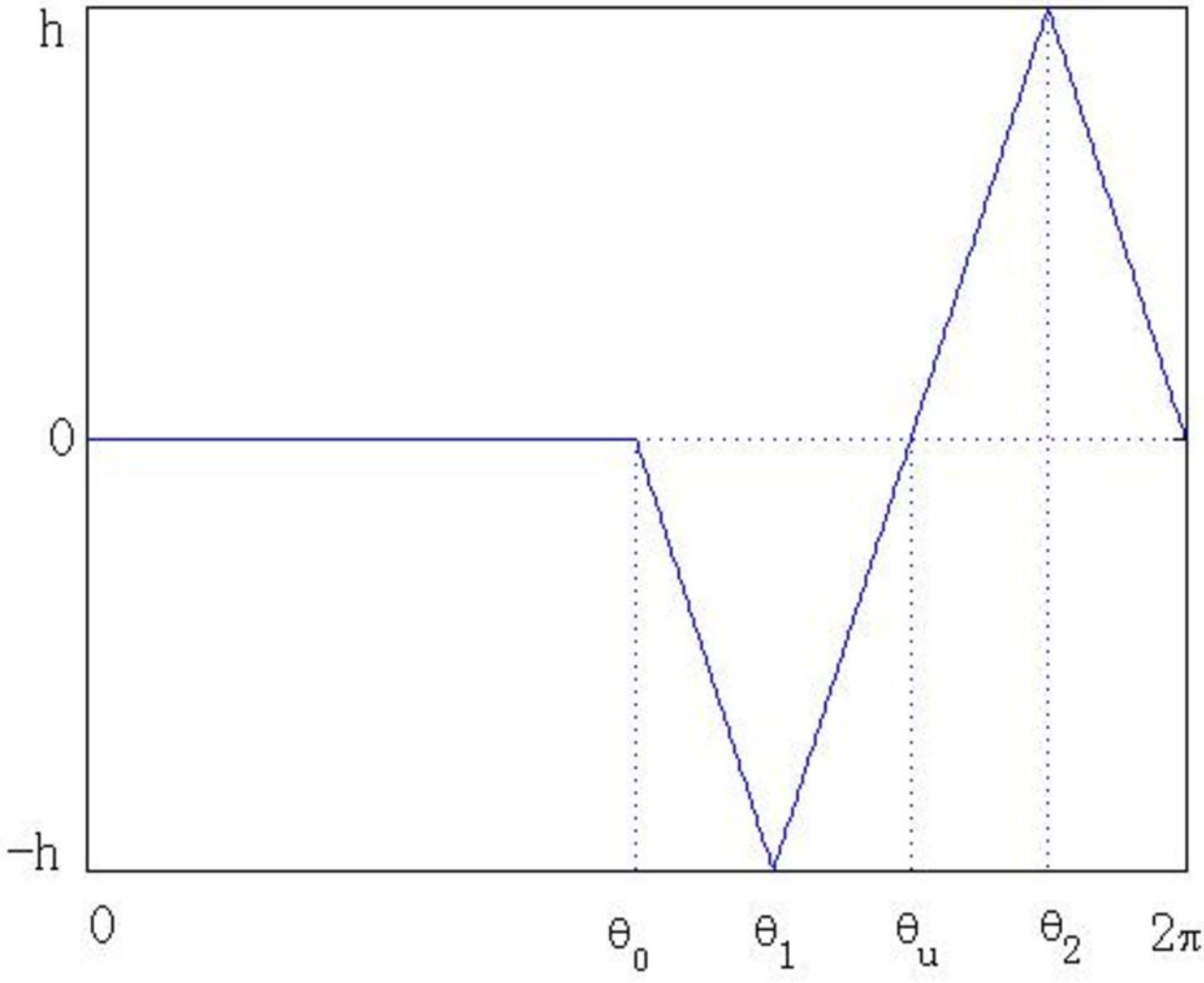
h
0
−h
0
θ0
θ1
θu
θ2
2π

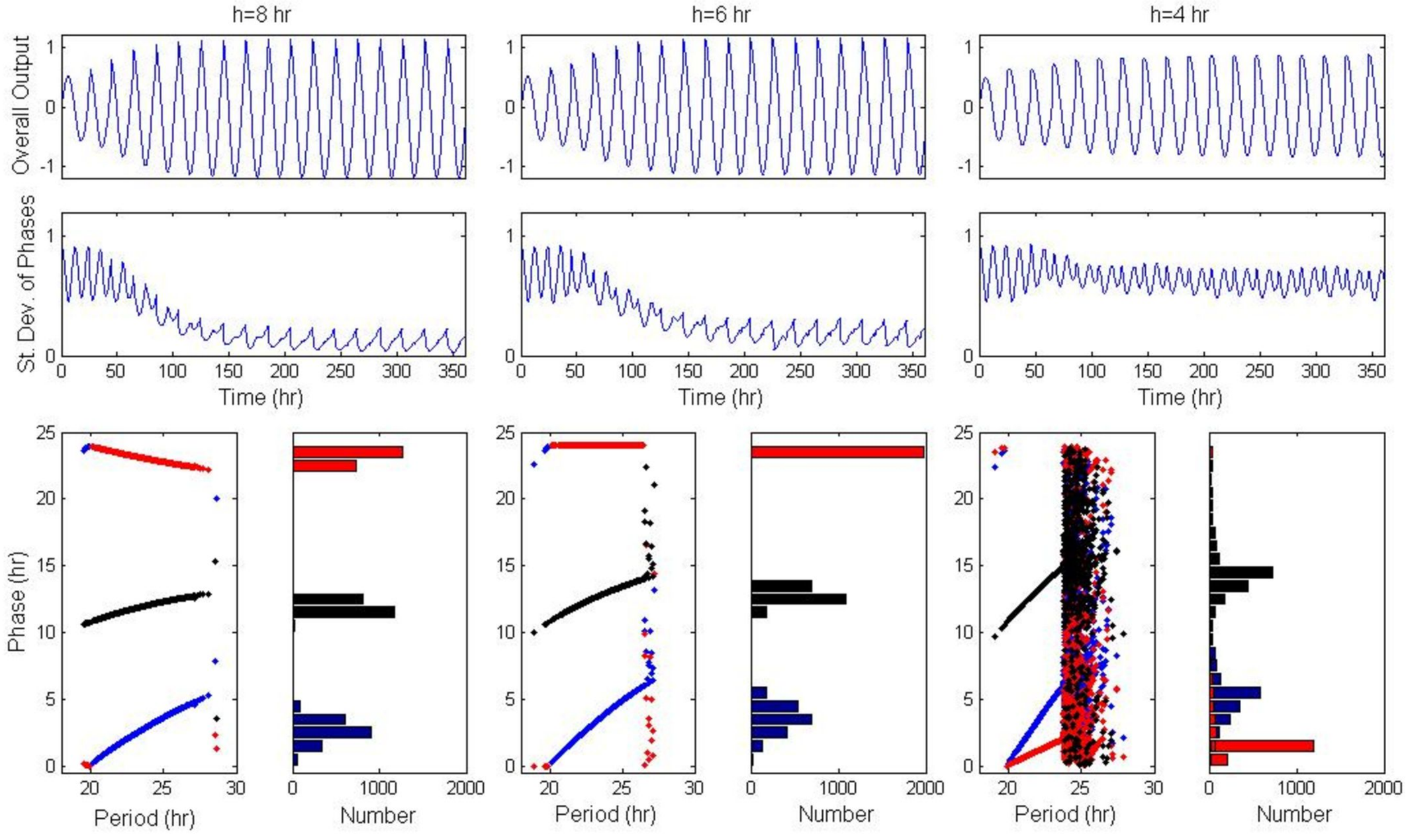
h=8 hr
h=6 hr
h=4 hr
Overall Output
St. Dev. of Phases
Time (hr)
Phase (hr)
Period (hr)
Number

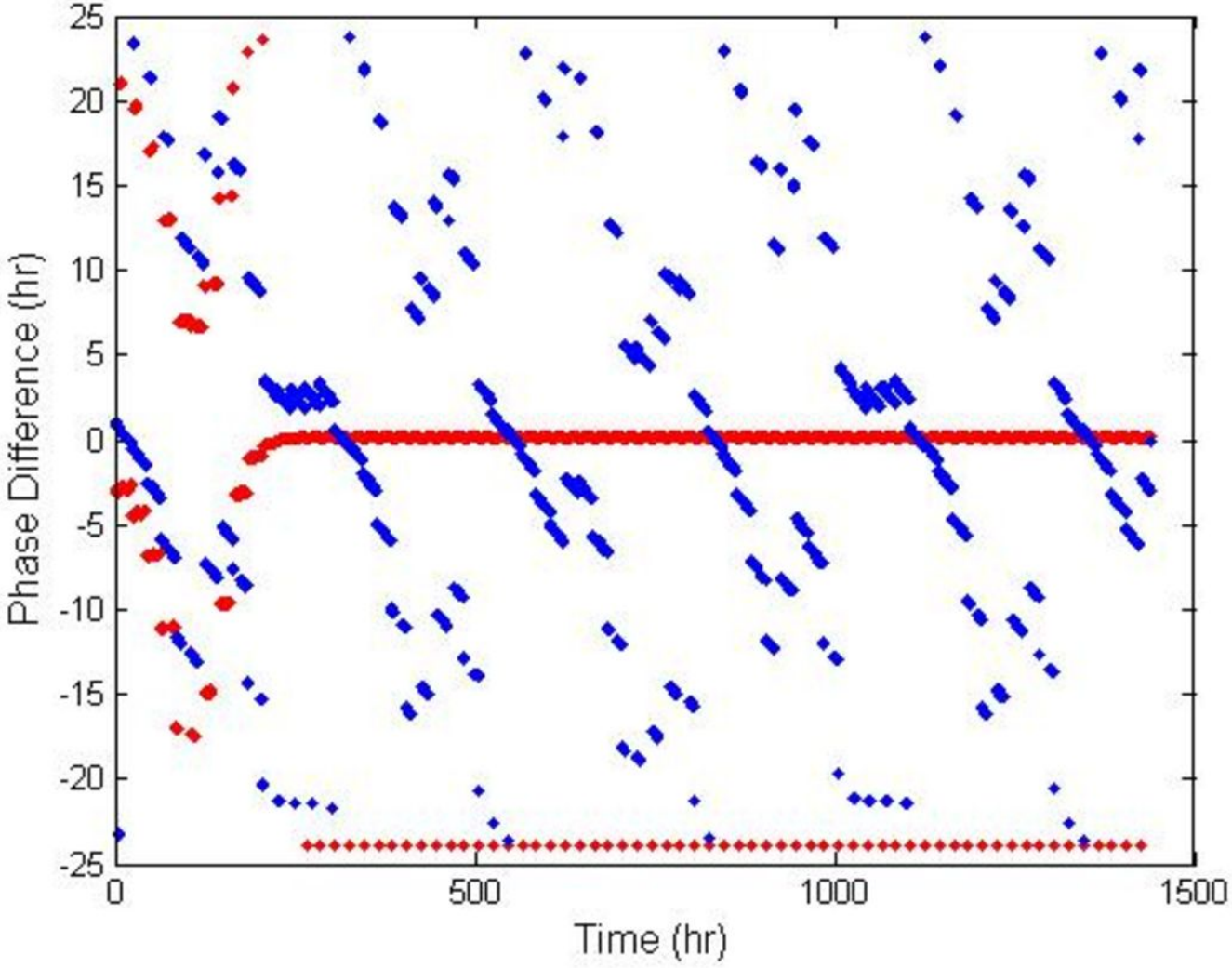
25
20
15
10
5
0
-5
-10
-15
-20
-25
Phase Difference (hr)
0
500
1000
1500
Time (hr)

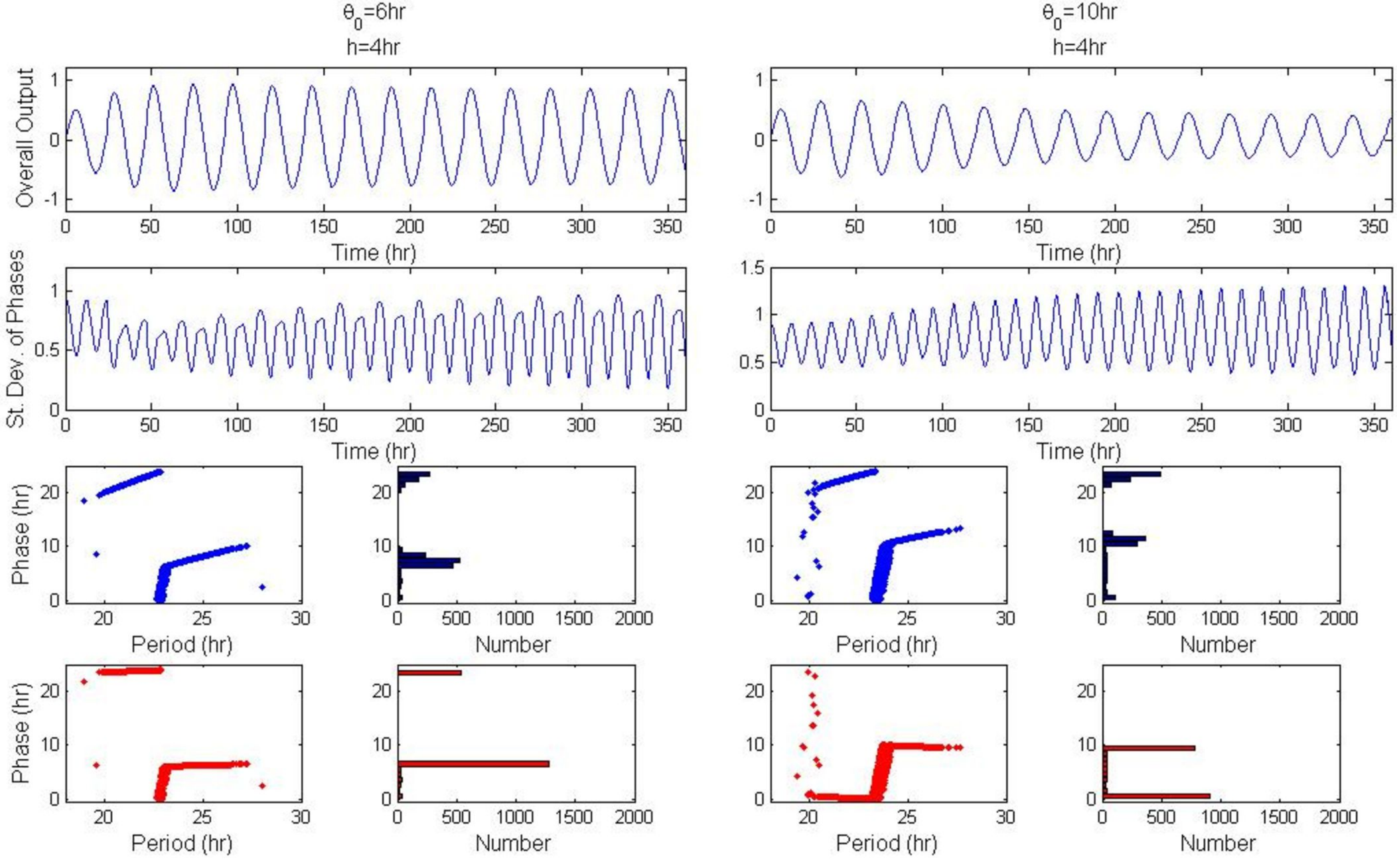
θ0=6hr
h=4hr
θ0=10hr
h=4hr
Overall Output
Time (hr)
St. Dev. of Phases
Phase (hr)
Period (hr)
Number

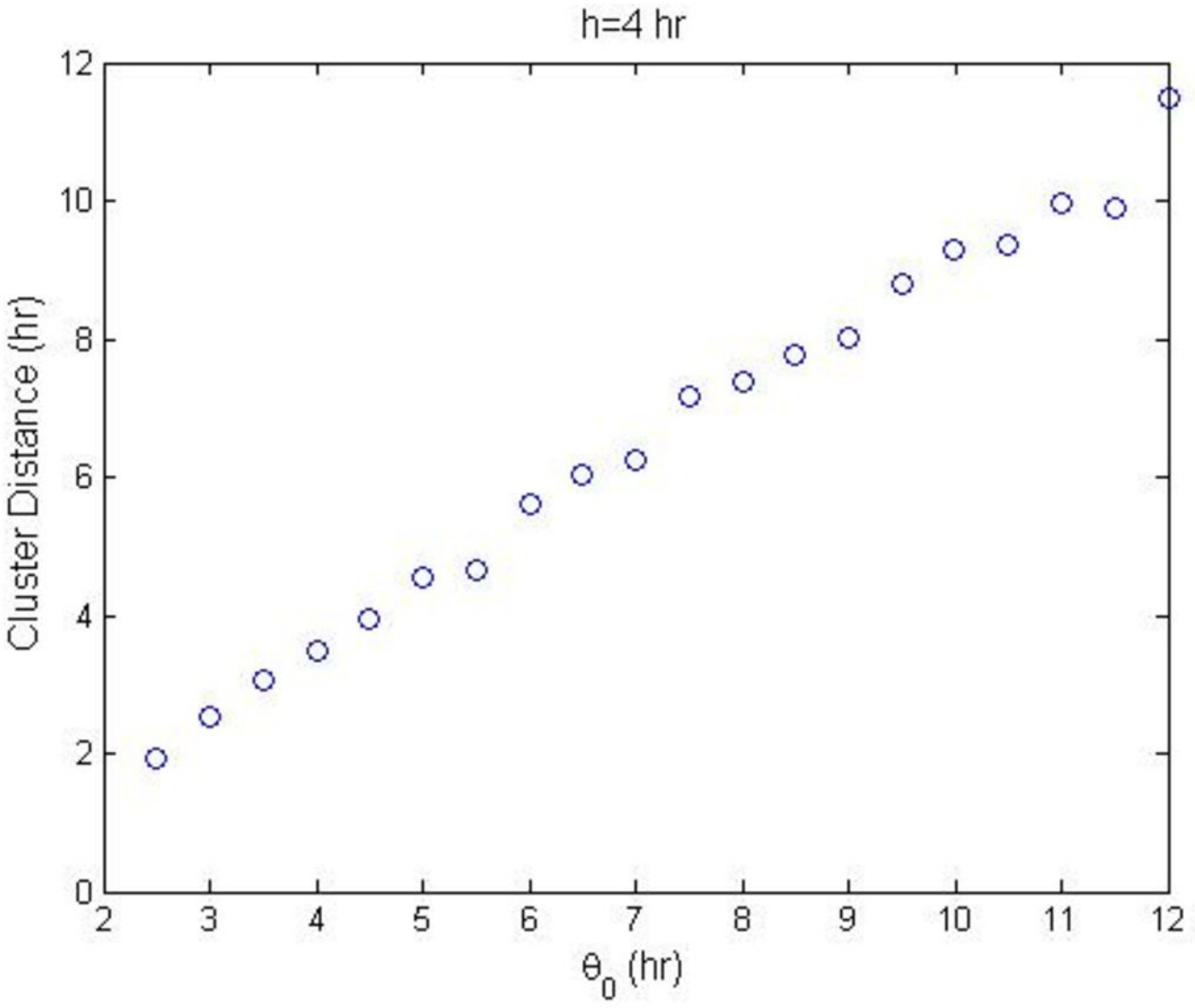
h=4 hr
Cluster Distance (hr)
θ0 (hr)
0
2
4
6
8
10
12
2
3
4
5
6
7
8
9
10
11
12

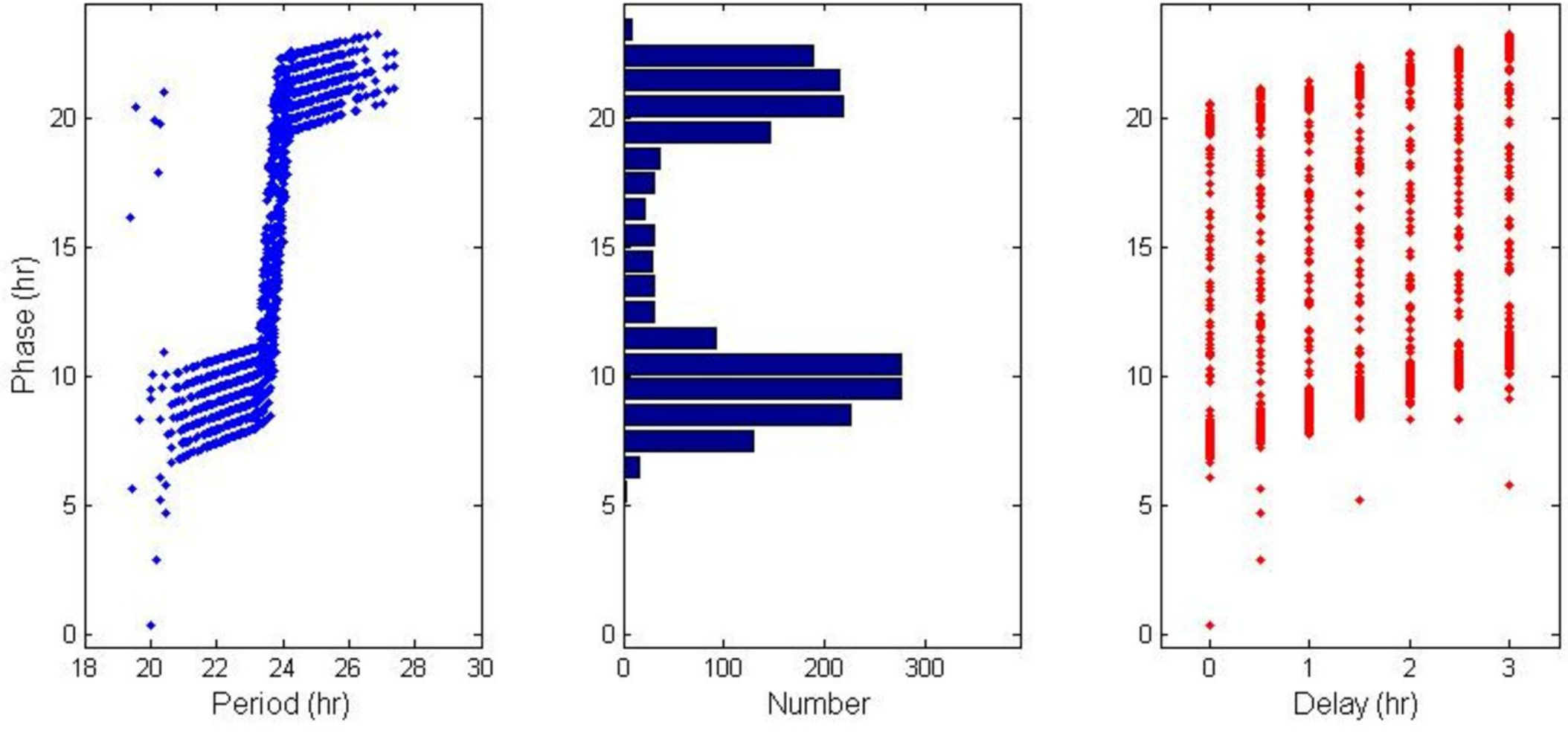
Phase (hr)
Period (hr)
Number
Delay (hr)

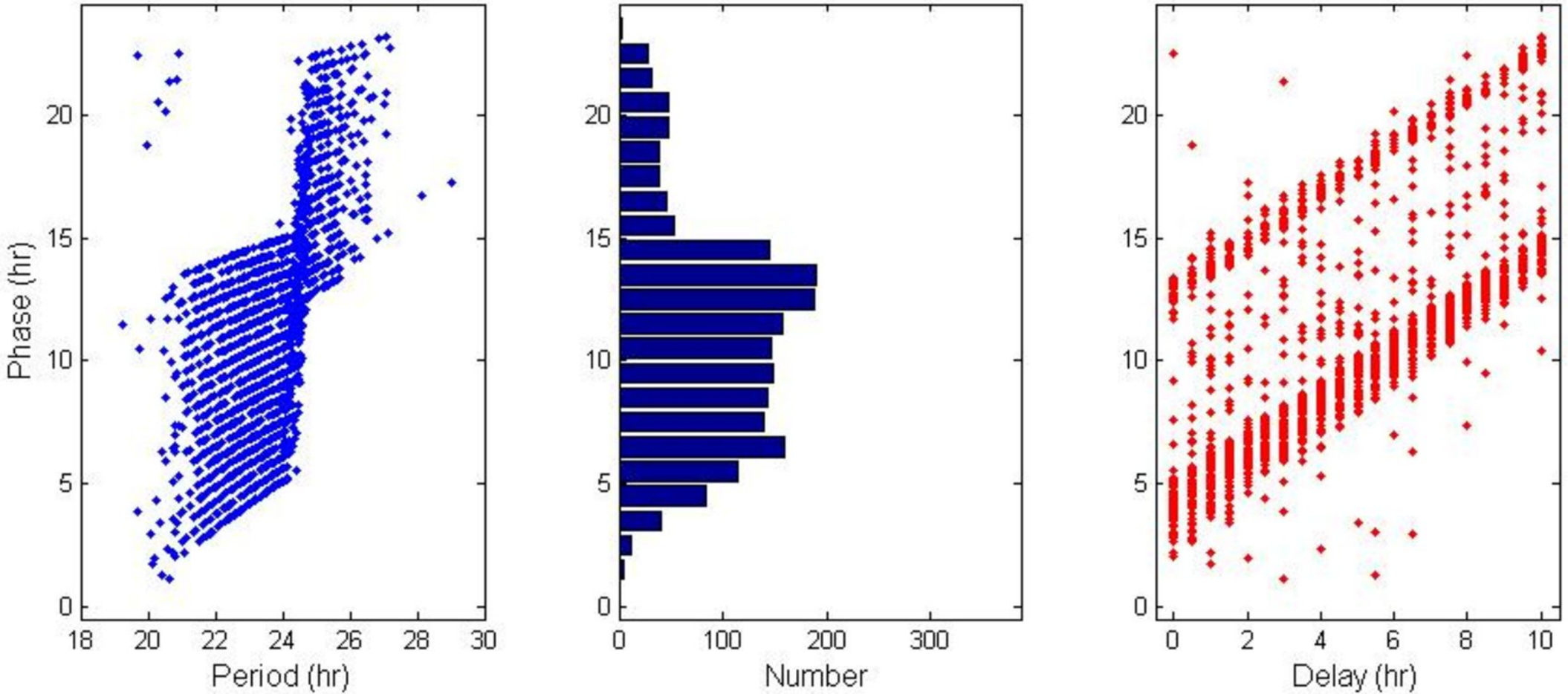
Phase (hr)
Period (hr)
Number
Delay (hr)